Journal of Catalysis 283 (2011) 45–54

Contents lists available at ScienceDirect

Journal of Catalysis

journal homepage: www.elsevier.com/locate/jcat

The roles of carbide and hydride in oxide-supported palladium nanoparticles for alkyne hydrogenation

Min Wei Tew [a], Markus Janousch [b], Thomas Huthwelker [b], Jeroen A. van Bokhoven [a,b,*]

[a] ETH Zurich, Institute for Chemical and Bioengineering, 8093 Zurich, Switzerland
[b] Paul Scherrer Institute, 5232 Villigen, Switzerland

ARTICLE INFO

Article history:
Received 14 April 2011
Revised 28 June 2011
Accepted 30 June 2011
Available online 16 August 2011

Keywords:
Selective partial hydrogenation
1-Pentyne
Oxide-supported palladium nanoparticles
Palladium hydrides
Palladium carbide
Effect of particle size
Pd L_3 edge in situ X-ray absorption near edge structure

ABSTRACT

Particle size affects the activity and selectivity to partial hydrogenation of 1-pentyne over oxide-supported palladium nanoparticles. Larger particles are intrinsically more selective because of the weaker bond strength of 1-pentene. In situ X-ray absorption near edge structure (XANES) at the Pd L_3 edge revealed the formation of a carbide-like phase as soon as the catalyst is exposed to alkyne, irrespective of particle size. The newly formed phase prevented hydride formation. Surface poisoning of the palladium carbide by alkyne is responsible for the constantly high selectivity, up to almost complete conversion. At almost 100% conversion, all catalysts show low selectivity. The lack of significant pentyne adsorption on the surface causes pentene to undergo consecutive reactions, such as isomerization and complete hydrogenation. The structure of the catalyst was that of carbide-like phase and did not change. Palladium hydride did not form under any of the conditions. Exposure of a carbided catalyst to pure hydrogen leads to partial reversal of the structure. Hydride is not essential for complete hydrogenation to occur.

1. Introduction

Chemoselective hydrogenation is a common reaction in the chemical industry [1–4]. To achieve high yield, metal catalysts are generally modified, for example by lead poisoning of palladium to give a Lindlar catalyst [5,6], by adding dopants to Raney nickel [7], and by partial poisoning of the catalyst surface. Partial hydrogenation of alkynes is performed to remove traces of alkynes from streams of alkenes to prevent poisoning of the catalyst during polymerization and branching of poly-olefins [8,9]. Selective alkyne hydrogenation is characterized by the very strong adsorption of the alkyne, which poisons the surface and prevents the alkene from reacting further. The primary product from 1-alkyne is 1-alkene that converts into isomers and alkane in consecutive reactions.

The structure of palladium catalysts changes readily as the conditions to which the catalyst is exposed change. Palladium hydrides and carbides form easily, the latter of which forms after adsorption of alkynes [10,11]. Hydride formation in palladium catalysts depends on the size of the palladium particles [12–14]. Because the hydride is generally associated with unselective hydrogenation, variation in catalytic performance is expected [15,16]. In 1970s, Palczewska proposed the participation of hydrides in catalytic reactions and reviewed studies related to the catalytic reactivity of hydrogen on palladium and nickel hydride phases [17]. She concluded that the catalytic activity of palladium and nickel decreases when they transform into the respective hydride phases. Results of the hydrogenation of acetylene over supported palladium catalysts, with or without excess ethane, indicate that the formation of the β-hydride phase in large particles enhanced the full hydrogenation of acetylene [4,18–23], while surface hydrogen was much more selective to ethylene [24]. Similar results were obtained for alkynes of higher molecular weight [25–28]. Palladium particles smaller than 2 nm formed an α phase, which is more selective than the hydrogen-rich β phase [17,21,29–32]. Under low pressure, hydrogenation of alkene did not occur over a Pd(1 1 1) single crystal, because the hydrogen atoms diffused so deeply into the bulk that they were inaccessible to the adsorbed alkene. In contrast, alkene hydrogenation over palladium nanoparticles under low pressure occurred, because the weak binding of subsurface hydrogen meant that it was accessible to the adsorbed alkene [15]. The authors also concluded that β-hydride was more active and less selective to alkene than the α phase. The higher activity of the bulk-dissolved hydrogen than of the adsorbed surface hydrogen was confirmed by theoretical calculations [27,33,34].

During alkyne hydrogenation, adsorbed alkynes undergo hydrogenation/dehydrogenation reactions, during which palladium car-

* Corresponding author at: ETH Zurich, Institute for Chemical and Bioengineering, HCI E 127, Wolfgang-Pauli-strasse 10, 8093 Zurich, Switzerland.
E-mail address: j.a.vanbokhoven@chem.ethz.ch (J.A. van Bokhoven).

0021-9517/$ - see front matter © 2011 Elsevier Inc. All rights reserved.
doi:10.1016/j.jcat.2011.06.025

bide may form [10,11]. The formation of palladium carbide during acetylene hydrogenation at 100 °C was discussed as early as 1980s [35]. The decomposition of acetylene on the palladium surface produced carbon atoms, which penetrated the lattice and formed a solid solution of carbon in palladium. Two carbide phases, analogous to the α and β hydride phases, were observed when the palladium catalysts were exposed to acetylene at high temperature [10,36–38]. In situ XPS has revealed the formation of a surface carbide in bulk palladium during the selective hydrogenation of 1-pentyne [25]. Full hydrogenation occurred over a surface with bulk-dissolved hydride, indicating the instability of the carbide phase over which selective hydrogenation occurred. The formation of palladium carbide was also observed during acetoxylation of ethylene [39], selective hydrogenation of butadiene [40], and the selective hydrogenation of propyne [27,27] and 1-pentyne [11,25,26,41]. These studies showed that the structure of a catalyst is affected by the composition of the gas phase. Theoretical calculations showed that the formation of carbide is energetically feasible [27,42–44] and that carbides probably form at the steps-like sites at near-surface positions and diffuse toward the center of the palladium particles. Penetration to the bulk of the particle and formation of dense carbide structures are energetically unfeasible [27]. It was suggested that the carbide formed mainly in the near-surface region of the catalyst and that it completely suppressed the absorption of hydrogen [11,25,27] and, hence, increased selectivity. Palladium carbide has also been correlated with the loss of activity, stabilization of supported Pd catalysts, and high selectivity to alkene.

Despite results from different groups suggesting the formation of the palladium carbide during reactions [11,25], only very few characterization data of this species have been obtained under reaction condition, especially in case of nano-sized particles. In this work, we performed gas-phase hydrogenation of 1-pentyne over supported palladium nanoparticles and determined the structure of the palladium particles in situ by means of X-ray absorption near edge structure (XANES) at the Pd L_3 edge during selective and non-selective hydrogenation. The L_3 edge XANES probes the empty d density of states; thus, palladium in different oxidation states can be distinguished easily. Furthermore, hydrides can be identified in the near edge when there is a Pd–H antibonding state [14,45,46]. Because of the depth of penetration of high energy X-rays, XAS can be implemented under actual catalytic conditions [47]. The energy of the X-rays at the Pd L_3 edge (3175 eV) is moderate, which therefore required the adaptation of an in situ cell [48]. The measurements were taken at the PHOENIX I beamline of the Swiss Light Source. The lowest measurable palladium concentration in fluorescence mode was about 0.4 wt.%. The in situ spectroscopic data obtained enabled us to determine directly the role of hydride and carbide during selective and non-selective alkyne hydrogenation. We found that, irrespective of the palladium particle size, palladium carbide forms during the selective reaction and that, over time, the particles are completely carbided. Complete and selective hydrogenation occurred over this surface.

2. Experimental

2.1. Synthesis and characterization of silica-and alumina-supported palladium nanoparticles

The catalysts were prepared by incipient-wetness impregnation with either alumina or silica, as described elsewhere [14]. The catalysts are Pd/SiO_2-10.5, Pd/Al_2O_3-3.6, Pd/SiO_2-2.8, and Pd/Al_2O_3-1.3; the numbers at the end refer to the average particle size in nanometer, determined from scanning transmission electron microscopy, CO chemisorption (assuming a CO to Pd ratio of one), and X-ray absorption spectroscopy. All the catalysts had a Pd weight loading of 1.9%, as determined by inductive couple plasma mass spectrometry.

2.2. Gas-phase hydrogenation of 1-pentyne

The gas-phase hydrogenation of 1-pentyne was performed in a continuous-flow, fixed-bed tubular quartz reactor. The temperature difference of the oven was kept constant within 1 °C. The temperature at the bottom of the catalyst bed was measured with a chromel–alumel thermocouple. All the temperatures mentioned in the text refer to the measured temperature of the catalyst bed; these values at most varied by a few degrees. The catalyst was diluted with alumina or silica to give different dilution factors, i.e., the ratio between the amount in weight of pure catalyst and that of the respective diluents ranged from 100 to 400 to achieve different conversion levels. Sieved fractions ($45 < x < 60$ mesh) of the diluted catalyst, 0.05 g, were used in each experiment. A fresh batch of catalyst was used in each experiment. Prior to the catalytic reaction, the catalyst was reduced in situ at 2°/min to 150 °C and left for 1 h in a flow of pure hydrogen (30 mL/min). The catalyst was then cooled in pure hydrogen to the desired reaction temperature. 1-Pentyne (Fluka, 99% purity) in a stream of helium was introduced into the system and passed through a saturator at 0 °C. The 1-pentyne/helium flow was mixed with pure hydrogen before reaching the catalyst bed and the H_2/1-pentyne ratio adjusted. The reaction products were analyzed with an Agilent 6890A gas chromatograph (GC) equipped with an FID detector and an HP-5 (50 m × 0.32 mm) column. Under differential conditions, the reactions were performed at a constant reaction temperature of 80 °C. The sample dilutions were adjusted to give a conversion of around 10%. Conversion and selectivity were also determined as a function of hydrogen to 1-pentyne ratio and of increasing gas flow at 90 °C. When varying the hydrogen to 1-pentyne ratio, the flow rates of hydrogen were adjusted while the flow rates of helium, which contained the 1-pentyne, remained constant. When varying the gas flow, the total flow rates of helium-1-pentyne and of hydrogen were adjusted to maintain a H_2/1-pentyne ratio of 4. We did not find that the selectivity and conversion depend on the flow rate per min, but on the space time. The reactions were performed at a constant reaction temperature of 45, 75, and 100 °C to achieve different conversion levels. To identify the effect of increasing hydrogen partial pressure, an additional experiment was performed at 45 °C at a H_2/1-pentyne ratio of 10.

The TOF of the products was calculated using the following equation:

$$\mathrm{TOF}\ (\mathrm{s}^{-1}) = \frac{molecule_{product}/t}{n_{Surf.Pd}}, \tag{i}$$

where $n_{Surf.Pd}$ is the number of exposed palladium atoms as determined by CO chemisorption [49].

The selectivity (S) of the products was calculated using the following equation:

$$S_{product\ A} = \frac{A_{product\ A} \cdot W_{product\ A}}{mol_{all\ products}} \times 100\%, \tag{ii}$$

where A_i is the GC peak area and W_i the calibrated mol coefficient.

W_i was 1 for 1-pentene, trans-2-pentene, cis-2-pentene, and pentane and 0.5 for the oligomers, assuming that the oligomers consist mainly of hydrocarbons with 10 carbon atoms (C_{10}), as suggested by the retention time in the GC. The carbon balance was closed within the accuracy of the GC. Only at the initial stage of the reaction did alkyne adsorb irreversibly onto the catalyst.

2.3. Pd L_3 edge XANES

The structure of Pd/SiO_2-10.5 and Pd/SiO_2-2.8 during selective and non-selective hydrogenation of 1-pentyne was determined by means of Pd L_3 edge XANES. The measurements were taken at the X07MB (PHOENIX I) beamline of the Swiss Light Source with a double crystal Si(1 1 1) monochromator to select the energy of the incoming beam. High-order harmonics and thermal load of the monochromator crystals were reduced with a set of two plane rotatable mirrors. The fluorescent X-ray was detected by means of a silicon drift detector with an energy resolution of ~130 eV, placed at 90° to the incoming beam. The sample made an angle of 45° to both, beam and fluorescence detector. A very thin polymer window was attached to the detector to enable detection of the fluorescence of elements down to the carbon K edge [50]. The determination of each XANES spectrum took about 15 min. Two mirrors in a Kirkpatrick–Baez configuration provided a focal spot size of about 10 μm × 5 μm (horizontal × vertical). The incoming intensity of the beam (I_0) was monitored by a thin polyethylene foil covered by a 30-nm-thick nickel layer.

An aluminum plug-flow reactor, which can be heated to 400 °C, was used [48]. The reactor was placed in a stainless steel chamber which was vacuumed and refilled multiple times with nitrogen and helium to minimize the disturbance of air which could strongly affect the quality of the data. The chamber was eventually filled with 800 mbar of helium. The inlet and outlet of the reactor were fed through the chamber by Swagelok connections. The catalyst was diluted with silica (dilution factors from 2 to 5) to control the conversion. Sieved fractions ($45 < x < 60$ mesh) of the catalyst were packed in the plug-flow reactor and covered by a kapton film, 0.008 mm thick. Prior to the reaction, 4 mg catalyst was reduced in situ at 150 °C at 2°/min, left for 1 h, and cooled to the desired reaction temperature in pure hydrogen (30 mL/min). Spectra of the catalyst in pure hydrogen were collected at 150 °C and then at 40 and 100 °C respectively. 1-Pentyne (Fluka, 99% purity) was introduced into the system in a stream of helium, which passes through a saturator at 0 °C. The 1-pentyne/helium flow was mixed with pure hydrogen before reaching the catalyst bed, and the H_2/1-pentyne ratio was adjusted to 4. With the GC, conversion and selectivity were determined as functions of increasing gas flow in mL/min. XANES spectra of each flow were recorded. The reactions were performed at a constant reaction temperature of 40 or 100 °C. Measurements taken at the middle and at the bottom of the reactor yielded identical results. The XAS data were processed according to standard procedures using the XDAP software package (Version 2.3) [51].

3. Results

3.1. Activity and selectivity under different conditions

Fig. 1a shows the conversion under constant temperature of 80 °C. Nearly a constant conversion of 12% was obtained for Pd/SiO_2-10.5 and Pd/SiO_2-2.8 throughout the reaction. Both alumina-supported catalysts, particularly Pd/Al_2O_3-3.6, showed high activity at the beginning of the reaction and became deactivated over time. The reactivity of each catalyst was compared by means of TOF based on the number of adsorbed CO molecules (Fig. 1b). Pd/SiO_2-10.5, with the largest particle size, converted six times more pentyne than Pd/Al_2O_3-1.3 with the smallest particles and twice as much as Pd/SiO_2-2.8 per site per second. Due to the strong deactivation of Pd/Al_2O_3-3.6, it is not discussed. Fig. 1c–e show the corresponding selectivity of each catalyst to pentenes, pentane, and oligomers. Pd/SiO_2-10.5 showed a constantly higher selectivity to pentenes, while Pd/Al_2O_3-1.3 showed the lowest.

Fig. S1 (supporting information) shows the conversion of 1-pentyne on Pd/SiO_2-10.5 at different H_2/1-pentyne ratios at constant temperature of 90 °C. Starting from a H_2/1-pentyne ratio of 8, the conversion gradually decreased from 45% to 15% at decreasing H_2/1-pentyne ratio to 2. The corresponding selectivity to pentenes was 67% and 98%, while the selectivity to pentane was 20% and 2% respectively. The amount of oligomers remained below 5% regardless of the H_2/1-pentyne ratio used. Increasing the H_2/1-pentyne ratio back to 4 and then 6 led to conversion and selectivity trend which were similar to those values obtained during decreasing ratio. Our data confirmed that hydrogenation of alkyne usually shows a reaction order of between 0.5 and 1.5 in hydrogen and zero or even negative in alkyne [1,52–54]. Hydrogen adsorbs weakly compared to the alkyne, and the rate determining step is normally the addition of hydrogen to an adsorbed intermediate [55,56]. The hydrogen coverage is always very low and virtually the complete conversion range is the surface covered with alkyne.

3.2. Effect of temperature and conversion on activity and selectivity

Fig. 2a–d show the conversion and selectivity to pentenes, pentane, and oligomers over Pd/SiO_2-10.5 at 100 °C. Different levels of conversion were obtained by varying the flow and the dilution factor. The dilution factor means the ratio between the amounts in weight of pure catalyst and that of the respective diluents. At 10–30% conversion (Fig. 2a), the system showed about 92% selectivity to pentenes, 5% to oligomers, and 3% to pentane. The pentenes consisted of only 1-pentene (Fig. 2b). At almost 100% conversion, there was consecutive 1-pentene isomerization to cis- and trans-2-pentenes as well as full hydrogenation. The selectivity to 1-pentene eventually decreased to 0% (Fig. 2c and d). Fig. 2e and f give the data recorded at 45 °C. The conversion was below 5%, and the reaction was 100% selective to 1-pentene. The very low conversion made it difficult to detect small amount of products. Oligomer formation was lower than 5% in all cases. Fig. 3a and b give the reaction data under the same conditions as in Fig. 2e and f, with the exception that the H_2/1-pentyne ratio was 10. Increasing the hydrogen pressure led to twice as much conversion, but the selectivity did not change.

Fig. 4a–d gives the conversion and product selectivity of Pd/Al_2O_3-1.3 as a function of increasing gas flow at 100 °C. At conversion between 15 and 84% (Fig. 4a and b), the system showed 60 to 80% selectivity to pentenes, consisted mainly of 1-pentene. At 98% conversion, the selectivity to pentenes dropped to 48%; at >99% conversion, full hydrogenation occurred. At these high conversion levels, 1-pentene also converted to trans-2-pentene (23%) and cis-2-pentene (9%). At 100% conversion (Fig. 4c and d), full hydrogenation dominated (93% selectivity to pentane, 6% to oligomers, and 1% to pentenes). Fig. 4e and f gives the data of the reaction at 45 °C. The conversion was below 5%, and selectivity was about 82% to 1-pentene, 7% to pentane, and 11% to oligomers.

Based on the data in Figs. 2–4, selectivity versus conversion plots were constructed. Fig. 5a–d give the selectivity versus conversion plots of the other catalysts. Selectivity to 1-pentene, trans-2-pentene, and cis-2-pentene is referred to as selectivity to pentenes. Except for conversion below about 5%, all the catalysts showed constant selectivity to pentenes and pentane with near 100% conversion. Only at 100% conversion did full hydrogenation dominate and the selectivity to pentenes decreased to 0%. Moreover, under these conditions, 1-pentene isomerized. The selectivity to pentenes over Pd/SiO_2-10.5 was 90% compared to 80% over Pd/Al_2O-1.3. An increase of 10% in selectivity is extensive at such high level of selectivity. These plots indicate that selectivity is determined by the level of conversion and tends to be independent of temperature and that particle size affects the intrinsic selectivity to partial hydrogenation.

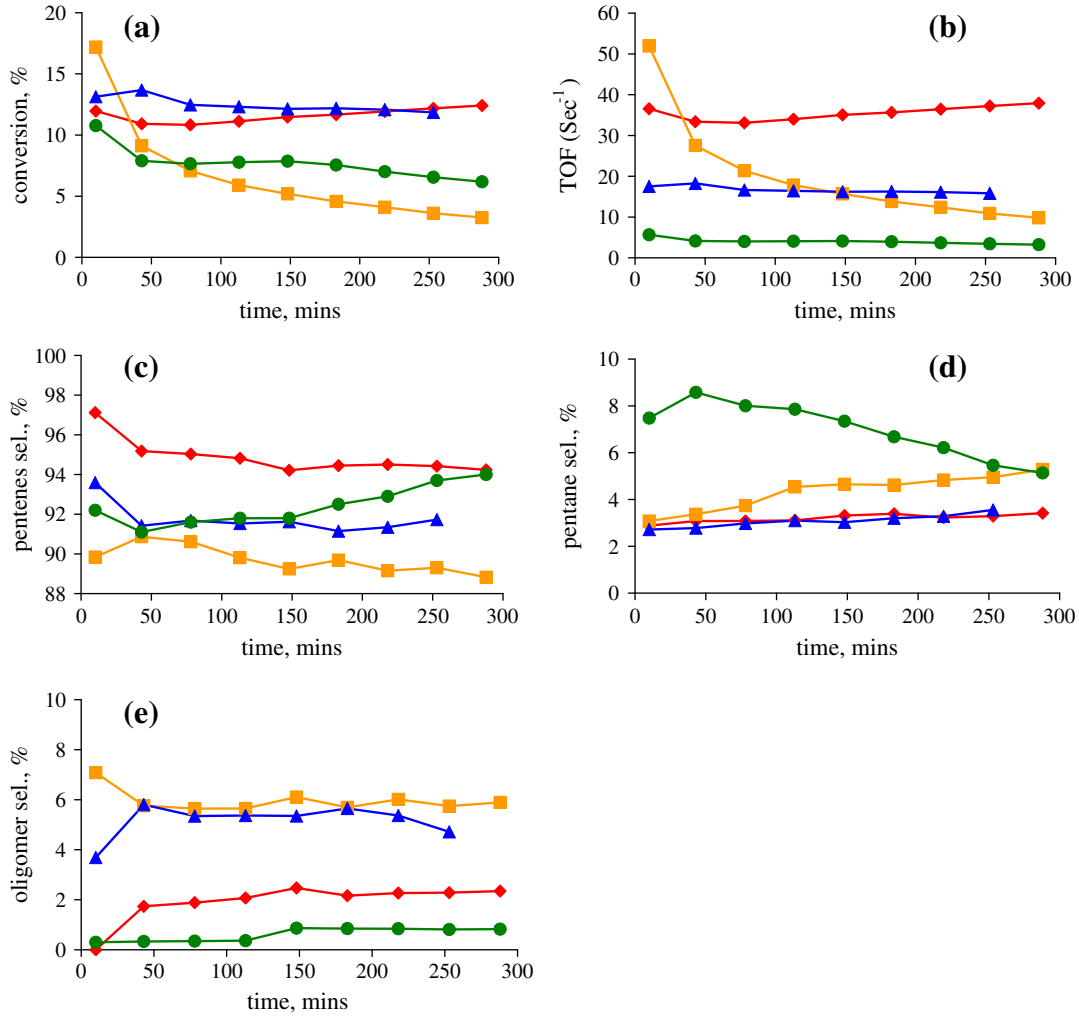

Fig. 1. (a) Conversion of 1-pentyne over (♦) Pd/SiO_2-10.5, (■) Pd/Al_2O_3-3.6, (▲) Pd/SiO_2-2.8, and (●) Pd/Al_2O_3-1.3 under differential conditions at 80 °C. (b) The corresponding TOF. Corresponding selectivity to (c) pentenes, to (d) pentane, and to (e) oligomers.

3.3. Pd L_3 edge XANES of reference samples

Fig. 6a shows the Pd L_3 edge XANES spectra of palladium nanoparticles, palladium hydride, and palladium carbide. The Pd L_3 edge XANES spectrum of the bare particles of Pd/SiO_2-10.5 was measured at 300 °C in He (Fig. 6, black [14]). It is characterized by an absorption edge at around 3175 eV together with an intense feature on the absorption edge, known as the whiteline. The typical hydride spectrum was obtained by exposing Pd/SiO_2-10.5 to pure hydrogen at 40 °C (Fig. 6, red). The edge shifts to higher energy, the intensity of the whiteline decreases, a new Pd–H antibonding state forms at around 3180 eV, and a change in the intensity at above 3185 eV occurs [14,45,46]. The spectrum of palladium carbide was measured under pure 1-pentyne, which leads to the formation of carbide (Fig. 6, pink) [10]. The edge shifts to higher energy and is very close to that of the hydride. Furthermore, the whiteline is significantly broader, and the intensity is between that of the bare particle and the hydride. Unlike the spectrum of hydride, no clear antibonding state was observed.

3.3.1. In situ Pd L_3 edge XANES

Table 1 lists the conversion and selectivity during the Pd L_3 edge experiments at 40 and 100 °C. The trends were similar to the previous catalytic data. For the experiments at 40 °C, conversion was low and selectivity to pentenes was high. The collected spectra, therefore, correspond to the catalyst structure in the selective region. For the experiments at 100 °C, both catalysts show high conversion and high selectivity to full hydrogenation (pentane). The spectra, therefore, correspond to the catalyst structure in the non-selective region (vide infra).

Figs. 7 and 8 show the spectra of Pd/SiO_2-2.8 and Pd/SiO_2-10.5 collected at 40 °C. The formation of hydride of both catalysts in H_2 was clearly indicated by the Pd–H antibonding state in the spectra. Upon exposure to the reactant mixture, the Pd–H antibonding state of Pd/SiO_2-10.5 and Pd/SiO_2-2.8 rapidly disappeared, indicating complete consumption of bulk hydrogen (Figs. 7 and 8, blue). At the same time, broadening of the whiteline occurred, indicating formation of a carbide-like phase. When the gas flow was increased to 57.1 mL/min, the spectra of both catalysts (Figs. 7 and 8, green) resembled that of the carbide-like phase (Fig. 6, pink): the whiteline became broader and intensity increased. These experiments indicate that formation of a carbide-like phase occurs in the selective region for both catalysts.

Figs. 9 and 10 show the spectra of Pd/SiO_2-10.5 and of Pd/SiO_2-2.8 at 100 °C. The formation of hydride of both catalysts was also found at 100 °C in H_2 (Figs. 9 and 10, red), although to lesser extent than at 40 °C. For both catalysts, the Pd–H antibonding state disappeared as soon as the system was exposed to the reactant mixture at 24.5 mL/min (Figs. 9 and 10, blue). Again for both catalysts,

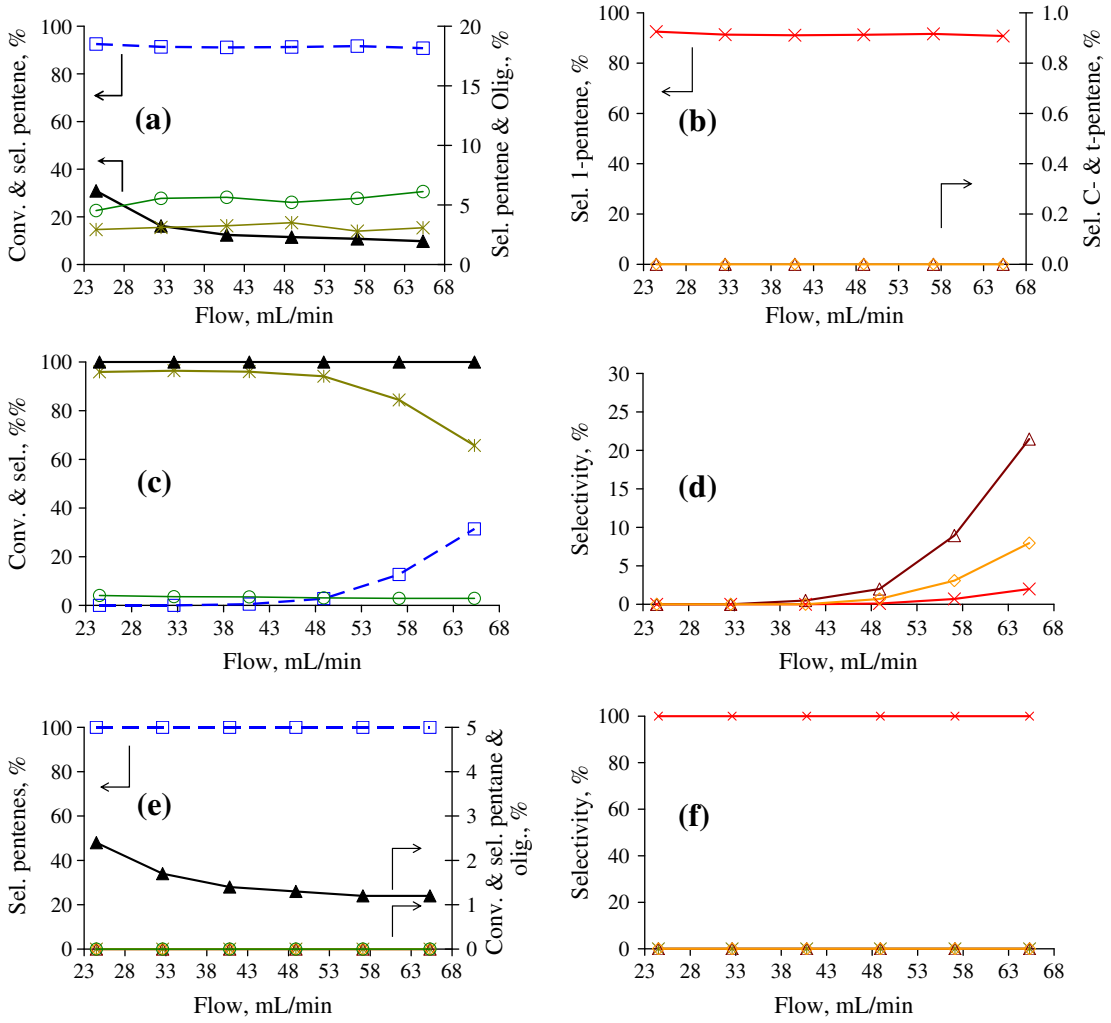

Fig. 2. Conversion (▲) and selectivity of pentenes (□), pentane (✳), oligomers (○), 1-pentene (×), t-2-pentene (△), and c-2-pentene (◇) as a function of total flow of Pd/SiO_2-10.5 at 100 °C and dilution factors of 100 (a and b) and 10 (c and d), and at 45 °C and a dilution factor of 100 (e and f).

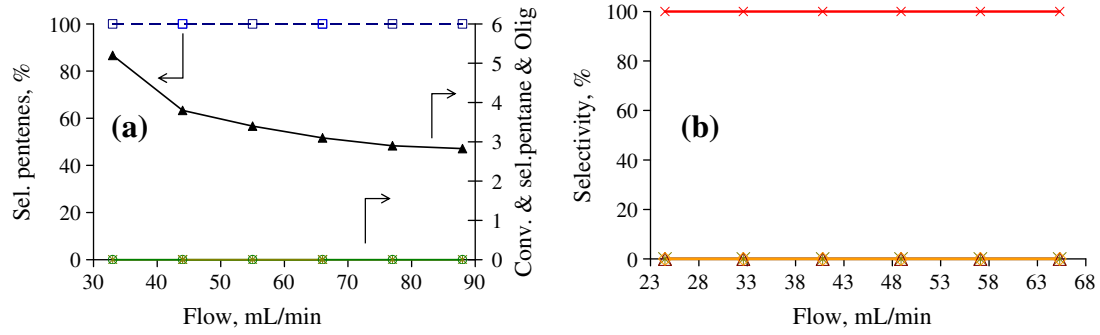

Fig. 3. (a and b) Conversion (▲) and selectivity of pentenes (□), pentane (✳), oligomers (○), 1-pentenes (×), t-2-pentene (△), and c-2-pentene (◇) as a function of total flow of Pd/SiO_2-10.5 at 45 °C and a dilution factor of 100 and a H_2/pentyne ratio of 10.

broadening of the whiteline and an increase in intensity were observed when the gas flow increased to 40.8 mL/min for Pd/SiO_2-2.8 or to 57.1 mL/min for Pd/SiO_2-10.5 (Figs. 9 and 10, green), which suggest the formation of a carbide-like phase. The formation of such phase occurs at 100 °C even in the presence of excess hydrogen at full conversion. These results were not affected by where the spectra were recorded, i.e., at the middle or bottom of the reactor. For Pd/SiO_2-10.5, the spectra collected after exposure to excess hydrogen at a hydrogen/1-pentyne ratio of 10 at 100 °C (gas flow = 42.5 mL/min) and to only 1-pentyne at 100 °C caused no significant difference in the spectra. Instead, the whiteline remained shifted and broader (Fig. 9, orange and pink), along with an increase in the intensity, indicating the stable presence of the carbide-like phase. For both catalysts, reexposure to pure hydrogen

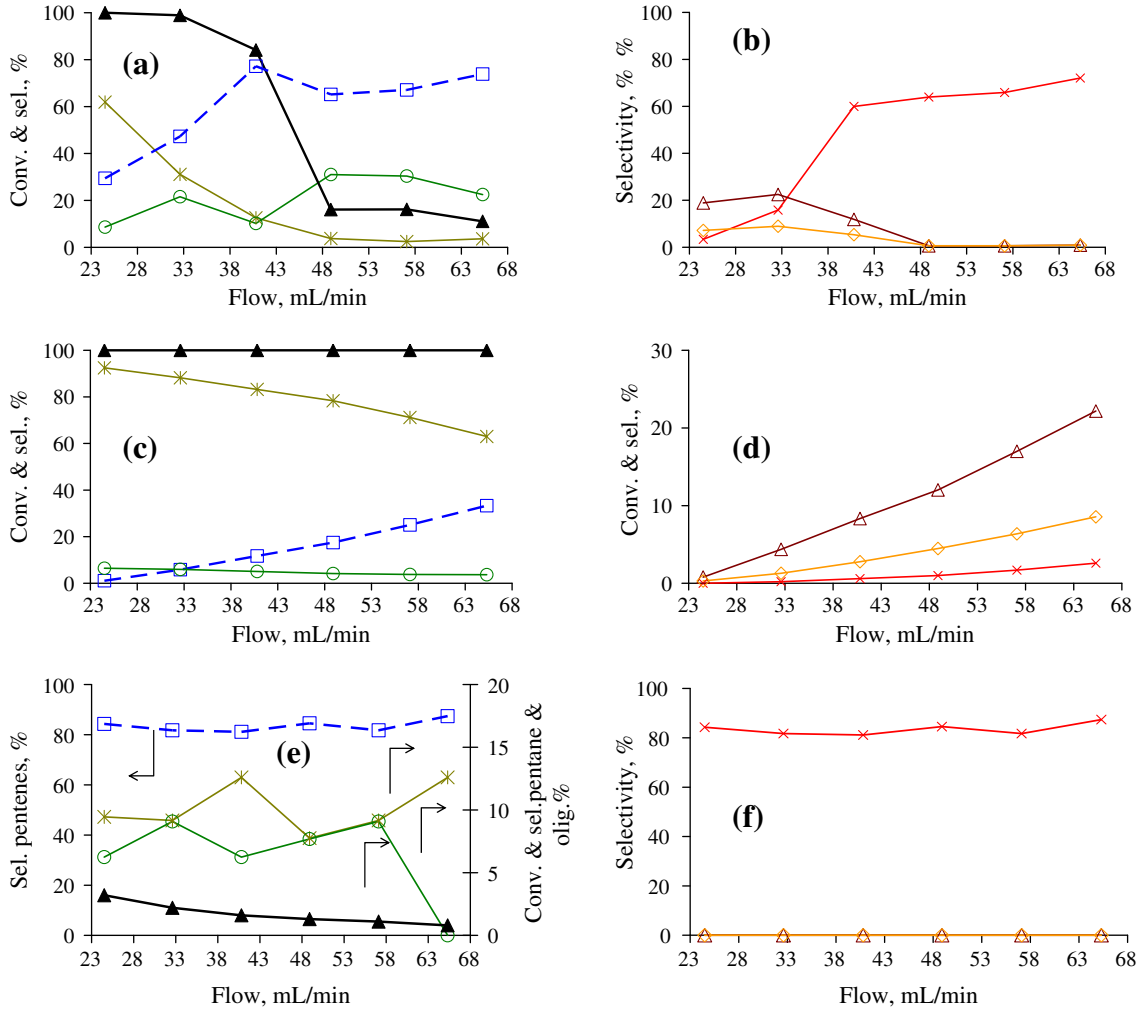

Fig. 4. Conversion (▲) and selectivity of pentenes (□), pentane (✳), oligomers (○), 1-pentenes (×), t-2-pentene (△), and c-2-pentene (◇) as a function of total flow of Pd/Al_2O_3-1.3 at 100 °C at dilution factors of 300 (a and b) and 50 (c and d), and at 45 °C at a dilution factor of 100 (e and f).

(Figs. 9 and 10, cyan) caused the weak reappearance of the Pd–H antibonding feature, indicative of hydride. Its intensity remained low, indicating that only some of the carbide-like phase was converted into hydride.

4. Discussion

4.1. Selectivity versus conversion

Selectivity of hydrogenation of alkynes over palladium-based catalysts is generally attributed to the thermodynamic effect: alkynes adsorb stronger than the corresponding alkenes [57–60]. The selectivity of the reaction is essentially determined by the relative surface coverage of adsorbed alkyne respectively alkene on the catalyst. A sharp decrease in selectivity occurred only at close to full conversion of the alkyne, because of the ability of alkene to re-adsorb [1]. The low alkyne coverage enables the fast reaction of alkene, such as in isomerization and full hydrogenation, which are faster than alkyne hydrogenation [1,8,61]. During complete hydrogenation over palladium black, the subsurface carbon undergoes hydrogenation [11,25]. In contrast, the structure of the nanoparticles did not change during the transition from the selective to the unselective regime. The constant and small amount of pentane at all conversion levels probably originated from the presence of a small amount of pentenes, which did not desorb from the surface but underwent direct consecutive hydrogenation.

4.2. Reaction mechanism and effect of particle size

During the hydrogenation of alkynes, they adsorb strongly on the catalyst surface. The first formed olefin may desorb or undergo consecutive reactions, such as hydrogenation and isomerization (Fig. 11) [3]. Competition between desorption of the pentene and the consecutive reactions to pentane determine the intrinsic selectivity of the catalyst. High selectivity to pentene is expected when k_4, k_5, and k_6, which refer to the extent, to which pentane and oligomers form from 1-pentyne but without the formation of desorbed pentene. When $k_1/k_{-1} \gg k_3/k_{-3}$, strong and preferential adsorption of 1-pentyne poisons the surface, effectively displacing the pentene and inhibiting its re-adsorption. Only when the concentration of 1-pentyne is low, can the pentene undergo consecutive reactions such as isomerization (k_6) and full hydrogenation (k_5) (Figs. 2–5).

The intrinsic selectivity to partial hydrogenation in the selective regime was affected by the particle size of palladium. Large particles (Pd/SiO_2-10.5) were intrinsically more selective to partial hydrogenation. Smaller particles were more selective to the formation of pentane and oligomers. DFT calculations gave the adsorption energy of acetylene and ethylene on various transition metal surfaces; they uniquely correlate with the energy of the carbon-

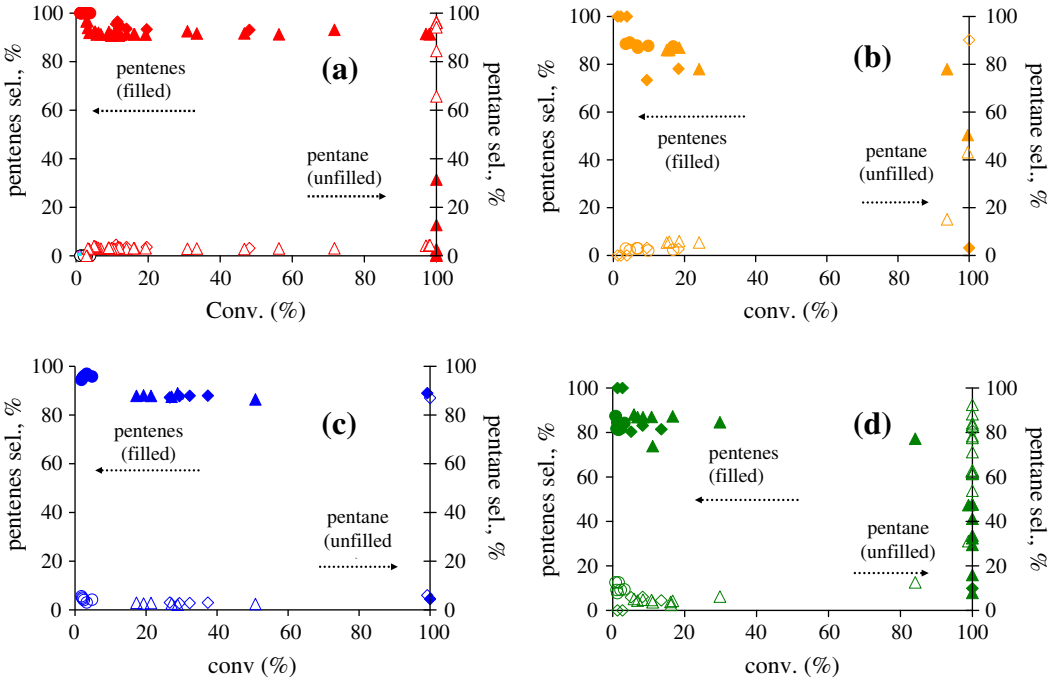

Fig. 5. Selectivity to pentenes and pentane versus conversion plot of: (a) Pd/SiO_2-10.5, (b) Pd/Al_2O_3-3.6, (c) Pd/SiO_2-2.8, and (d) Pd/Al_2O_3-1.3. Selectivity versus conversion plots include data from experiments performed at a reaction temperature of 45 °C (●),75 °C (♦), or 100 °C (▲).

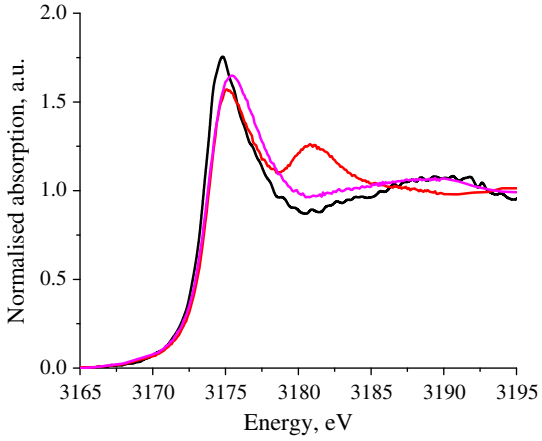

Fig. 6. Pd L_3 edge spectra of Pd/SiO_2-10.5, at 300 °C in He (black, [14]) and at 40 °C in H_2 (red) and in 1-pentyne (pink). (For interpretation of the references to color in this figure legend, the reader is referred to the web version of this article.)

Table 1
Kinetic data for the Pd L_3 edge experiments at 40 and 100 °C.

		Pd/SiO_2-10.5		Pd/SiO_2-2.8	
		(A) 40 °C	(B) 100 °C	(C) 40 °C	(D) 100 °C
24.5 mL/min	Conversion (%)		100	33	100
	Selectivity (%)				
	Pentane		87	5	93
	Pentene		10	80	0
	Oligomers		3	15	7
40.8 mL/min	Conversion (%)	12	95		100
	Selectivity (%)				
	Pentane	0	64		80
	Pentene	100	31		13
	Oligomers	0	5		7
57.1 mL/min	Conversion (%)	10	93	12	
	Selectivity (%)				
	Pentane	0	56	0	
	Pentene	100	38	83	
	Oligomers	0	6	17	

surface bond, as determined from the adsorption energy of methyl groups [57]. An energy range for metals and alloys with an optimal combination of high activity and selectivity was proposed. Surfaces in this energy range were predicted to show weak binding with ethylene but strong binding with acetylene, thus enabling partial hydrogenation. Both ethylene and acetylene showed weaker bonding on palladium with subsurface carbon and hydrogen than on clean palladium, and such catalysts are generally more selective. Nevertheless, palladium with subsurface hydrogen had a significantly weaker effect on the selectivity and reactivity on the palladium surface than on the surface with subsurface carbon. Selective hydrogenation occurred on a carbided surface, showing that the strong pentyne bonding is responsible for the selective hydrogenation. We found that the larger particles showed higher selectivity. Larger particles may adsorb more weakly as long as the surface is covered with alkynes; the weaker adsorption of alkenes has a stronger effect and, thus a higher selectivity. Weaker adsorption of poisonous species may enhance the rate. In addition to a different adsorption strength, the selectivity to pentenes is influenced by the relative amount of planes and edges and corner atoms and the kind of exposed surface of the palladium particles. Big particles have larger extended planes than small particles, which have more edge and corner sites. Terminal alkyne can adsorb on the surface in a parallel or perpendicular manner, while internal alkyne can only bond in a parallel state, assuming facile removal of the alkynic hydrogen [62]. Large particles thus favor 2-pentyne hydrogenation while for 1-pentyne hydrogenation, the differences were less significant. In terms of activity, our TOF results agree with those obtained for the hydrogenation of 1-butyne over oxide-supported palladium catalysts, where the reaction activity decreased as the particle size decreased [63,64].

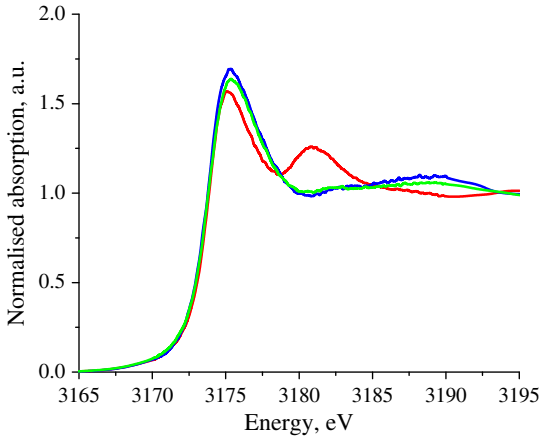

Fig. 7. Pd L_3 edge spectra of Pd/SiO_2-10.5 at 40 °C in H_2 (red), during reaction at 40.8 mL/min (blue) and 57.1 mL/min (green). The spectra correspond to kinetic data in Table 1 (A). (For interpretation of the references to color in this figure legend, the reader is referred to the web version of this article.)

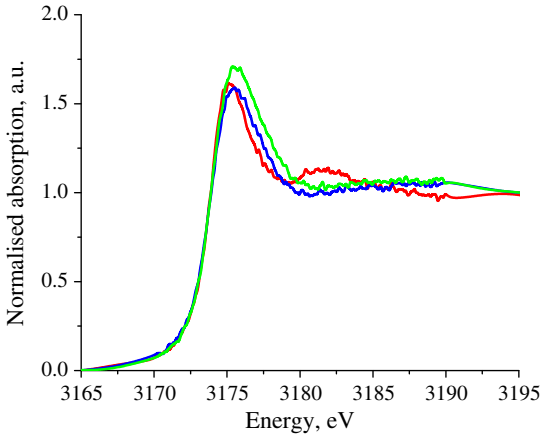

Fig. 8. Pd L_3 edge spectra of Pd/SiO_2-2.8 at 40 °C in H_2 (red), during reaction at 24.5 mL/min (blue) and 57.1 mL/min (green). The spectra correspond to kinetic data in Table 1 (C). (For interpretation of the references to color in this figure legend, the reader is referred to the web version of this article.)

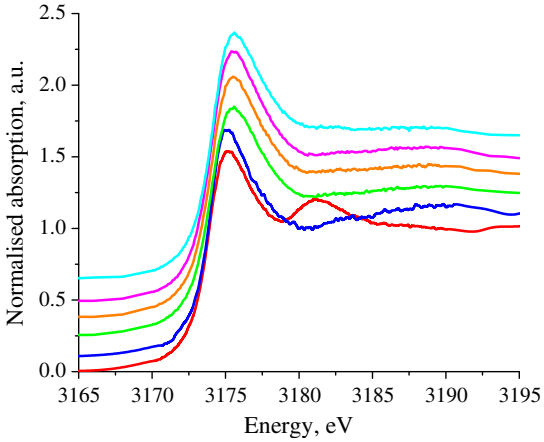

Fig. 9. Pd L_3 edge spectra of Pd/SiO_2-10.5 at 100 °C in H_2 (red), during reaction at 24.5 mL/min (blue) and 57.1 mL/min (green). In excess hydrogen at a H_2/-pentyne ratio of 10 (orange) at 100 °C. In 1-pentyne at 100 °C (pink) and reexposed to H_2 at 40 °C (cyan). The spectra correspond to kinetic data in Table 1 (D). (For interpretation of the references to color in this figure legend, the reader is referred to the web version of this article.)

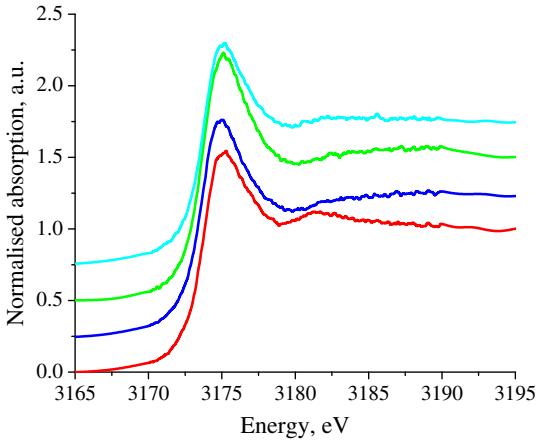

Fig. 10. Pd L_3 edge spectra of Pd/SiO_2 -2.8 at 100 °C in H_2 (red), during reaction at 24.5 mL/min (blue) and 40.8 mL/min (green). Reexposed to H_2 at 100 °C (cyan). The spectra correspond to kinetic data in Table 1 (B). (For interpretation of the references to color in this figure legend, the reader is referred to the web version of this article.)

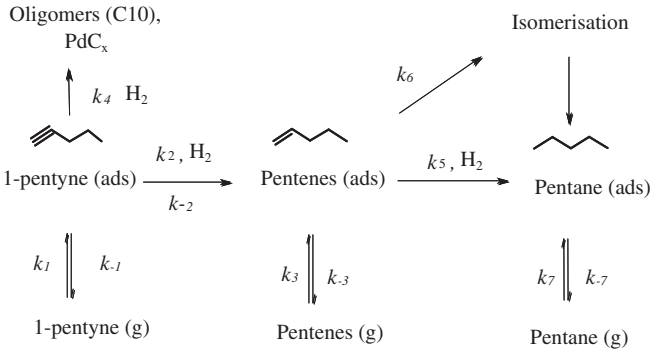

Fig. 11. Reaction mechanism during hydrogenation of alkynes [26].

4.3. The structure of palladium during reaction

The results of this study indicated that the exposure of fully reduced catalysts to hydrogen always produced hydrides [14,45,46]. As soon as the catalyst was exposed to 1-pentyne, the hydrides transformed into a disordered, carbide-like phase, even in the presence of excess hydrogen. We only observed the formation of the carbide-like phase after the exposing the catalyst to pentyne, not pentene. Scheme 1 describes the structures that form after consecutive exposure of the catalysts to different gas mixtures. Alkynes bond very strongly to the palladium surface and readily undergo hydrogenation and dehydrogenation, which gradually fully transform the palladium particles into a palladium carbide-like phase, probably starting at the (sub) surface. Reexposure of the carbide-like phase to hydrogen for 1 h (Figs. 9 and 10) restores the hydride structure only to a small extent, indicating the stability of the nano-sized carbide-like phase, as opposed to the instability of subsurface carbide in massive palladium [11,25]. The presence of hydrogen does not hinder the dehydrogenation of alkyne, which enables the incorporation of carbon into the palladium structure; under 1-pentyne and hydrogen, the carbide-like phase also forms. Although it takes some time for the particles to be carbided, selective hydrogen is found on fully occurs over particles with the carbide-like phase. The structure of our nanoparticles did not change when changing to the unselective regime. Even though the presence of hydride is often associated with complete hydrogenation, it is not essential for complete hydrogenation to occur.

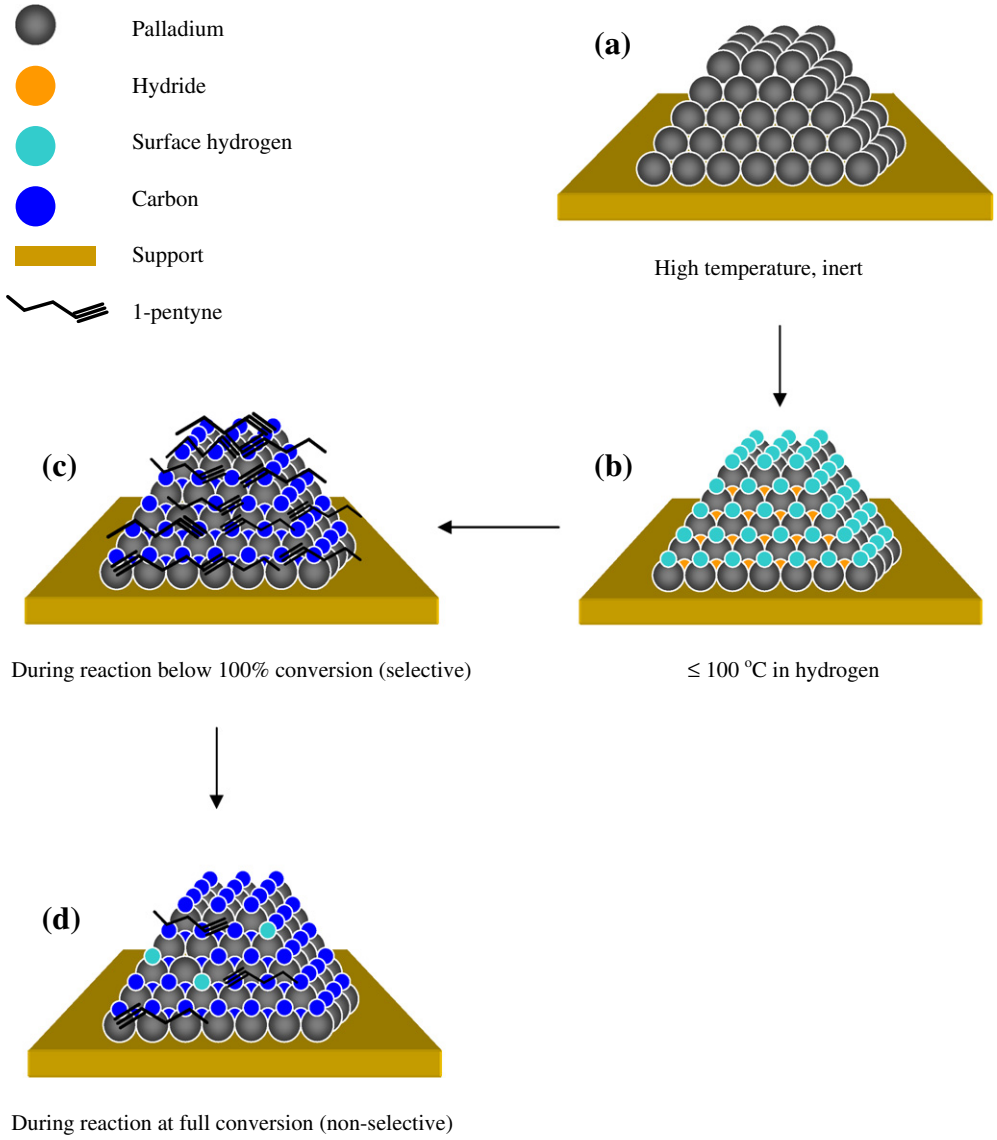

Scheme 1. Structures that form after consecutive exposure of the catalysts to different gas mixtures: (a) bare palladium nanoparticles, (b) formation of surface hydrogen and hydride under hydrogen, (c) formation of palladium carbide-like phase during the selective hydrogenation, and (d) arbide during non-selective hydrogenation.

5. Conclusions

During the hydrogenation of 1-pentyne, the alkyne poisons the surface of palladium nanoparticles and effectively displaces the pentene to desorb from the surface. The inhibition of the reaction of pentenes leads to suppressed conversion and high selectivity, the latter of which depends on particle size; the larger particles are more selective and have a higher TOF. The intrinsic selectivity depends on the relative bond strength of the alkynes and alkenes. Pentene isomerization and full hydrogenation dominate when the concentration of 1-pentyne is low enough for pentene to undergo secondary reactions. This occurs at high conversion. Alkyne undergoes hydrogenation and dehydrogenation, which gradually transform the palladium particles into a palladium carbide-like phase. Surface poisoning by alkyne of the palladium carbide-like phase is responsible for the high selectivity below 95% conversion. The nano-sized carbided palladium particles did not change in the non-selective regime, and full hydrogenation occurred over the carbided particles. Exposure of the carbided catalyst to pure hydrogen leads to subtle changes in the structure. Hydride was not detected during reaction. Full hydrogenation can also occur in the absence of hydride.

Acknowledgments

The authors acknowledge the Swiss National Science Foundation (SNF) for financial support. The Pd L_3 edge experiments were performed on the X07MB (PHOENIX I) beamline at the Swiss Light Source, Paul Scherrer Institute, Villigen, Switzerland. The authors thank Dr. Jeffrey T. Miller of the Chemical Technology Division of the Argonne National Laboratory, United States for the samples, the workshop of the ETH Zurich for constructing the in situ plug-flow reactor, and Erich DeBoni and Beat Meier of the Swiss Light Source for optimizing the plug-flow reactor.

Appendix A. Supplementary material

Supplementary data associated with this article can be found, in the online version, at doi:10.1016/j.jcat.2011.06.025.

References

[1] G.C. Bond, Metal-Catalysed Reactions of Hydrocarbons, Springer, New York, 2005.

[2] S.A. Nikolaev, L.N. Zanaveskin, V.V. Smirnov, V.A. Averyanov, K.L. Zanaveskin, Russ. Chem. Rev. 78 (2009) 231.
[3] Á. Molnár, A. Sárkány, M. Varga, J. Mol. Catal. A: Chem. 173 (2001) 185.
[4] A. Borodziński, G.C. Bond, Catal. Rev. Sci. Eng. 48 (2006) 91.
[5] H. Lindlar, Helv. Chim. Acta 35 (1952) 446.
[6] H. Lindlar, R. Dubuis, Org. Synth. 5 (1973) 880.
[7] L.W. Covert, R. Connor, H. Adkins, J. Am. Chem. Soc. 54 (1932) 1651.
[8] A.N.R. Bos, K.R. Westerterp, Chem. Eng. Process. 32 (1993) 1.
[9] A. Borodziński, Catal. Lett. 63 (1999) 35.
[10] S.B. Ziemecki, G.A. Jones, D.G. Swartzfager, R.L. Harlow, J. Am. Chem. Soc. 107 (1985) 4547.
[11] D. Teschner, E. Vass, M. Hävecker, S. Zafeiratos, P. Schnörch, H. Sauer, A. Knop-Gericke, R. Schlögl, M. Chamam, A. Wootsch, A.S. Canning, J.J. Gamman, S.D. Jackson, J. McGregor, L.F. Gladden, J. Catal. 242 (2006) 26.
[12] P.C. Aben, J. Catal. 10 (1968) 224.
[13] M. Boudart, Adv. Catal. 20 (1969) 153.
[14] M.W. Tew, J.T. Miller, J.A. van Bokhoven, J. Phys. Chem. C 113 (2009) 15140.
[15] A.M. Doyle, S.K. Shaikhutdinov, S.D. Jackson, H.J. Freund, Angew. Chem. Int. Ed. 42 (2003) 5240.
[16] W. Palczewska, in: Z. Paal, P.G. Menon (Eds.), Hydrogen Effects in Catalysis, Marcel Dekker, New York, 1988, p. 373.
[17] W. Palczewska, Adv. Catal. 24 (1975) 245.
[18] A. Borodziński, R. Duś, R. Frak, A. Janko, W. Palczewska, in: G.C. Bond, P.B. Wells, F.C. Tompkins (Eds.), Proceedings of the 6th International Congress on Catalysis, London, July 12–16, 1976, Chemical Society, London, 1977.
[19] A. Borodziński, A. Janko, React. Kinet. Catal. Lett. 7 (1977) 163.
[20] G. Carturan, G. Facchin, G. Cocco, S. Enzo, G. Navazio, J. Catal. 76 (1982) 405.
[21] C.E. Gigola, H.R. Aduriz, P. Bodnariuk, Appl. Catal. 27 (1986) 133.
[22] H.R. Aduriz, P. Bodnariuk, M. Dennehy, C.E. Gigola, Appl. Catal. 58 (1990) 227.
[23] Q.W. Zhang, J. Li, X.X. Liu, Q.M. Zhu, Appl. Catal. A 197 (2000) 221.
[24] N.A. Khan, S. Shaikhutdinov, H.J. Freund, Catal. Lett. 108 (2006) 159.
[25] D. Teschner, J. Borsodi, A. Wootsch, Z. Révay, M. Hävecker, A. Knop-Gericke, S.D. Jackson, R. Schlögl, Science 320 (2008) 86.
[26] D. Teschner, J. Borsodi, Z. Kis, L. Szentmiklosi, Z. Revay, A. Knop-Gericke, R. Schlogl, D. Torres, P. Sautet, J. Phys. Chem. C 114 (2010) 2293.
[27] M. Garcia-Mota, B. Bridier, J. Perez-Ramirez, N. Lopez, J. Catal. 273 (2010) 92.
[28] B. Bridier, N. Lopez, J. Perez-Ramirez, Dalton Trans. 39 (2010) 8412.
[29] G.C. Bond, P.B. Wells, The poisoning of a palladium catalyst by mercury vapor, in: Proceedings of 2nd International Congress on Catalysis, Technip, Paris, 1960, p. 1159.
[30] A. Sarkany, A.H. Weiss, L. Guczi, J. Catal. 98 (1986) 550.
[31] H. Arnold, F. Dobert, J. Gaube, in: G. Ertl, H. Knözinger, J. Weitkamp (Eds.), Handbook of Heterogenous Catalysis, vol. 5, VCH, Germany, 1997, p. 3266.
[32] W.J. Kim, J.H. Kang, I.Y. Ahn, S.H. Moon, J. Catal. 226 (2004) 226.
[33] A. Michaelides, P. Hu, A. Alavi, J. Chem. Phys. 111 (1999) 1343.
[34] V. Ledentu, W. Dong, P. Sautet, J. Am. Chem. Soc. 122 (2000) 1796.
[35] A. Frackiewicz, A. Janko, Acta Crystallogr. Sect. A 34 (1978) S377.
[36] J. Stachurski, A. Frackiewicz, J. Less-Common Metals 108 (1985) 249.
[37] S.B. Ziemecki, G.A. Jones, J. Catal. 95 (1985) 621.
[38] J.A. Mccaulley, Phys. Rev. B: Condens. Matter Mater. Phys. 47 (1993) 4873.
[39] A.H. Zaidi, Appl. Catal. 30 (1987) 131.
[40] T. Ouchaib, J. Massardier, A. Renouprez, J. Catal. 119 (1989) 517.
[41] D. Teschner, Z. Revay, J. Borsodi, M. Havecker, A. Knop-Gericke, R. Schlogl, D. Milroy, S.D. Jackson, D. Torres, P. Sautet, Angew. Chem. Int. Ed. 47 (2008) 9274.
[42] N. Seriani, F. Mittendorfer, G. Kresse, J. Chem. Phys. 132 (2010) 024711.
[43] P. Sautet, F. Cinquini, Chemcatchem 2 (2010) 636.
[44] I.V. Yudanov, K.M. Neyman, N. Rosch, Phys. Chem. Chem. Phys. 6 (2004) 116.
[45] A.V. Soldatov, S. Dellalonga, A. Bianconi, Solid State Commun. 85 (1993) 863.
[46] T. Kubota, Y. Kitajima, K. Asakura, Y. Iwasawa, Bull. Chem. Soc. Jpn. 72 (1999) 673.
[47] J.A. van Bokhoven, T. Ressler, F.M.F. De Groot, G. Knop-Gericke, in: B.M. Weckhuysen (Ed.), *In situ* Spectroscopy of Catalysts, American Scientific Publishers, 2004, p. 123.
[48] N. Weiher, E. Bus, B. Gorzolnik, M. Moller, R. Prins, J.A. van Bokhoven, J. Synchrotron Radiat. 12 (2005) 675.
[49] A. Borodziński, Langmuir 13 (1997) 5613.
[50] A.M. Flank, G. Cauchon, P. Lagarde, S. Bac, M. Janousch, R. Wetter, J.M. Dubuisson, F.M. Idir, T. Langlois, D. Moreno, D. Vantelon, Nucl. Instrum. Methods Phys. Res. Sect. B 246 (2006) 269.
[51] D.C. Koningsberger, B.L. Mojet, G.E. van Dorssen, D.E. Ramaker, Top. Catal. 10 (2000) 143.
[52] C.A. Hamilton, S.D. Jackson, G.J. Kelly, R. Spence, D. de Bruin, Appl. Catal. A 237 (2002) 201.
[53] L. Brandaõ, D. Fritsch, A.M. Mendes, L.M. Madeira, Ind. Eng. Chem. Res. 46 (2007) 377.
[54] G.C. Bond, D.A. Dowden, N. Mackenzie, Trans. Faraday Soc. 54 (1958) 1537.
[55] G. Webb, in: C.H. Bamford, C.F.H. Tipper (Eds.), Comprehensive Chemical Kinetics, vol. 21, Elsevier, Amsterdam, 1978, p. 1.
[56] S. Bailey, F. King, in: R.A. Sheldon, H. van Bekkum (Eds.), Fine Chemicals through Heterogeneous Catalysis, Wiley, New York, 2001, p. 351.
[57] F. Studt, F. Abild-Pedersen, T. Bligaard, R. Sørensen, C. Christensen, J. Nørskov, Angew. Chem. Int. Ed. 120 (2008) 9439.
[58] J.B. Conn, G.B. Kistiakowsky, E.A. Smith, J. Am. Chem. Soc. 61 (1939) 1868.
[59] G.F. Taylor, S.J. Thomson, G. Webb, J. Catal. 12 (1968) 150.
[60] X.C. Guo, R.J. Madix, J. Catal. 155 (1995) 336.
[61] A.N.R. Bos, E.S. Bootsma, F. Foeth, H.W.J. Sleyster, K.R. Westerterp, Chem. Eng. Process. 32 (1993) 53.
[62] S.D. Jackson, C.A. Hamilton, G.J. Kelly, D. de Bruin, React. Kinet. Catal. Lett. 73 (2001) 77.
[63] J.P. Boitiaux, J. Cosyns, S. Vasudevan, Appl. Catal. 6 (1983) 41.
[64] J.P. Boitiaux, J. Cosyns, S. Vasudevan, Appl. Catal. 15 (1985) 317.